

# Appendix

<b>Table of contents</b>	<b>Page</b>
Appendix Table S1	2
Appendix Table S2	3
Appendix Table S3	4
Appendix Figure S1	5
Appendix Figure S2	7
Appendix Figure S3	8
Appendix Figure S4	9
Appendix Figure S5	11

**Appendix Table S1.** PHIP-1(H45A) binding proteins identified by yeast two-hybrid screen.

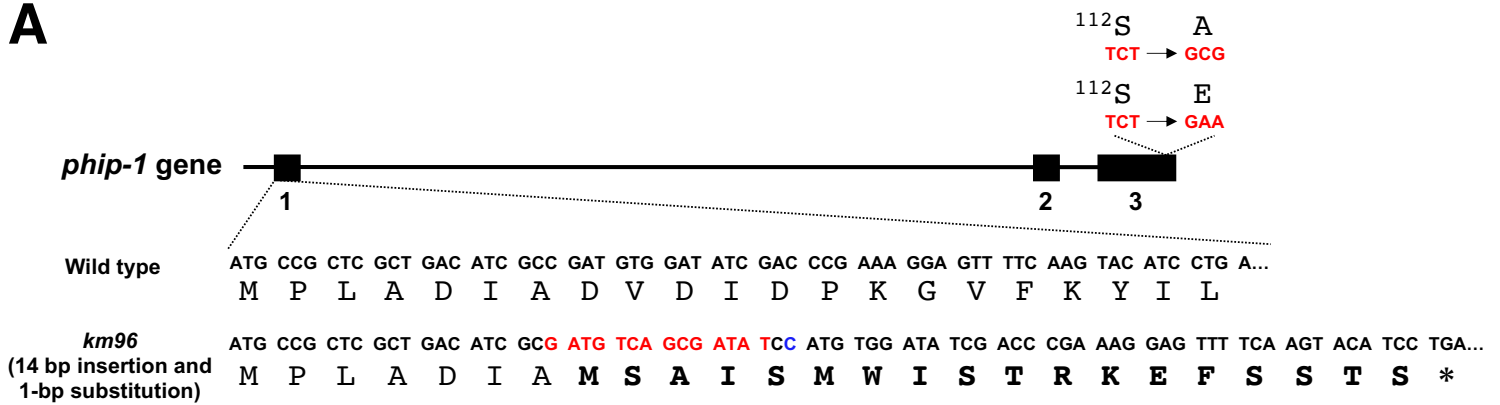
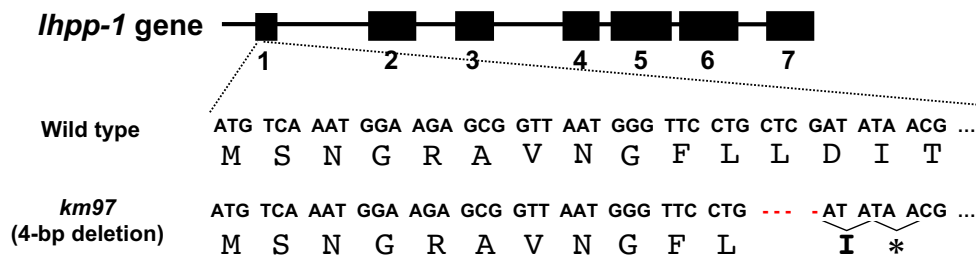
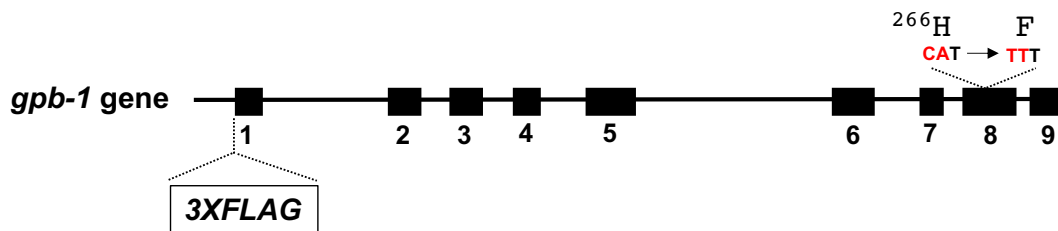
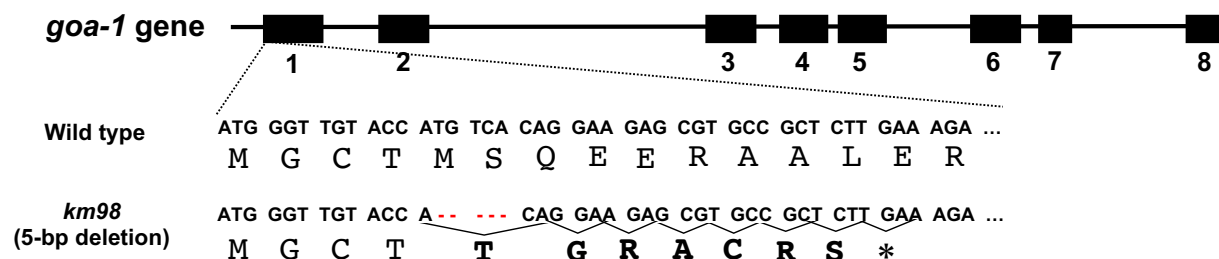
<b>Gene</b>	<b>Gene product</b>	<b>Number of colonies</b>
<i><b>gpb-1</b></i>	<b>G<math>\beta</math></b>	<b>1</b>
<i><b>gpd-2</b></i>	<b>GAPDH</b>	<b>1</b>
<i><b>gpd-3</b></i>		<b>12</b>
<i><b>gpd-4</b></i>		<b>8</b>
<i><b>unc-51</b></i>	<b>ULK homolog</b>	<b>1</b>

## Appendix Table S2. Strains used in this study.

Strain	Genotype
KU501	<i>juls76 II</i>
KU96	<i>phip-1(km96) I; juls76 II</i>
KU97	<i>juls76 II; lhpp-1(km97) V</i>
KU98	<i>goa-1(km98) I; juls76 II</i>
KU1461	<i>phip-1(km96) I; juls76 II; kmEx1461 [Punc-25::<i>phip-1</i>]</i>
KU1462	<i>phip-1(km96) I; juls76 II; kmEx1462 [Punc-25::<i>phip-1</i>(H45A)]</i>
KU1463	<i>juls76 II; kmEx1463 [Punc-25::<i>ndk-1</i>]</i>
KU1464	<i>juls76 II; kmEx1464 [Punc-25::<i>ndk-1</i>(H118N)]</i>
KU1465	<i>gpb-1(H266F) juls76 II</i>
KU1466	<i>phip-1(km96) I; gpb-1(H266F) juls76 II</i>
KU1467	<i>gpb-1(H266F) juls76 II; kmEx1463 [Punc-25::<i>ndk-1</i>]</i>
KU1468	<i>goa-1(km98) phip-1(km96) I; juls76 II</i>
KU455	<i>goa-1(Q205L) I; juls76 II</i>
KU1469	<i>goa-1(Q205L) I; gpb-1(H266F) juls76 II</i>
KU1343	<i>muls32 II</i>
KU1470	<i>muls32 II; unc-51(ks49) V</i>
KU1471	<i>phip-1(km96) I; muls32 II</i>
KU1472	<i>phip-1(S112A) I; muls32 II</i>
KU1473	<i>phip-1(S112E) I; muls32 II</i>
KU1474	<i>phip-1(S112E) I; muls32 II; unc-51(ks49) V</i>
KU1475	<i>gpb-1(H266F) muls32 II; unc-51(ks49) V</i>
KU1476	<i>muls32 II; lgg-2(tm6544) IV</i>
KU1477	<i>phip-1(km96) I; muls32 II; lgg-2(tm6544) IV</i>
KU1478	<i>3XFLAG::<i>gpb-1</i> juls76 II</i>
KU1479	<i>phip-1(km96) I; 3XFLAG::<i>gpb-1</i> juls76 II</i>
KU1480	<i>phip-1(km96) I; 3XFLAG::<i>gpb-1</i>(H266F) juls76 II</i>
KU1481	<i>juls76 II; unc-51(ks49) V</i>

## Appendix Table S3. DNA and RNA sequences.

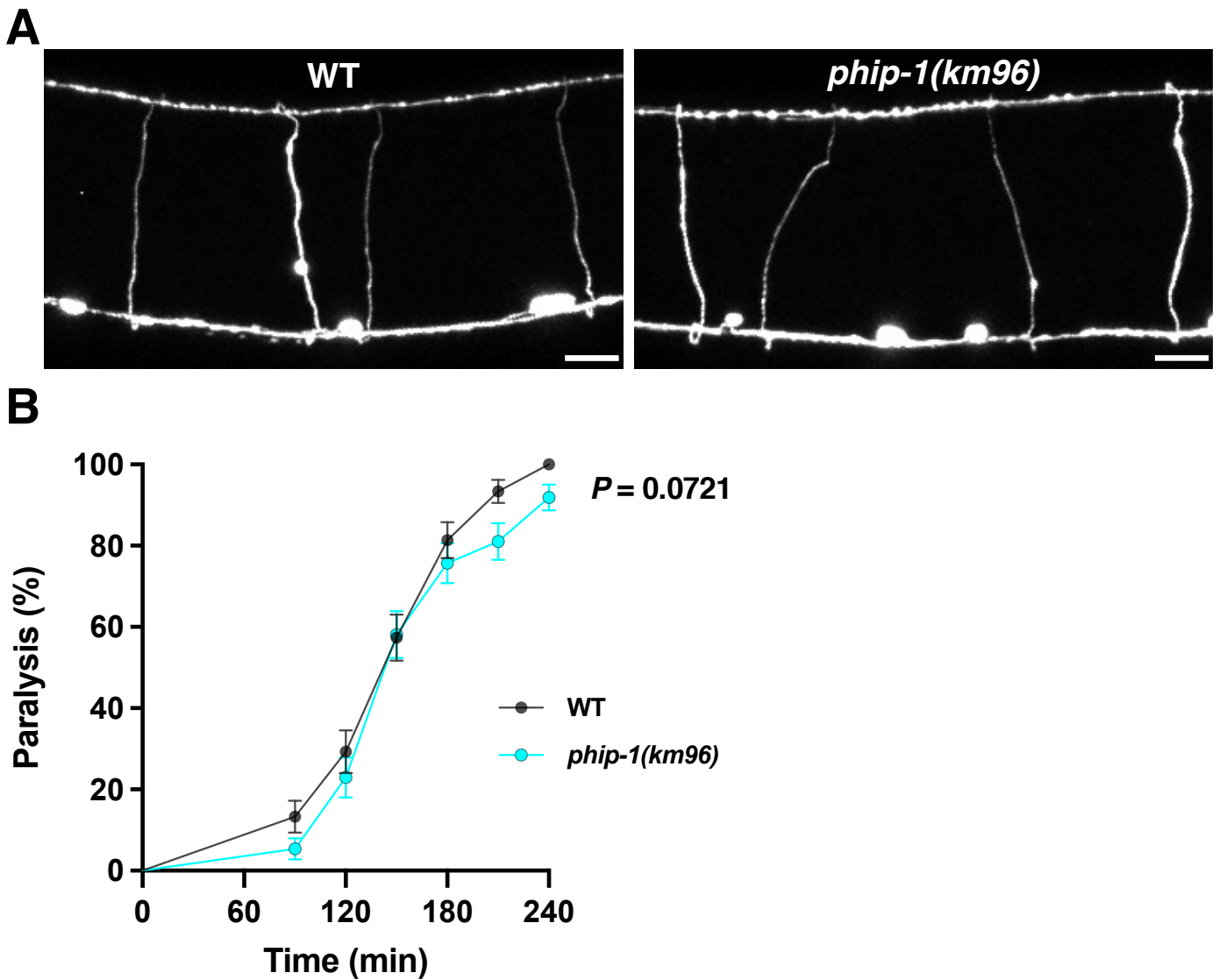
<i>phip-1(km96)</i>	crispr RNA	gcucgcugacaucgccgaugguuuuagagcuaugcu
	PCR primer for genotyping (forward)	ttatcacagtgtgagagcattggg
	PCR primer for genotyping (reverse)	gaagataatgaacaactgctctactc
<i>lhpp-1(km97)</i>	crispr RNA	aaacucccguuauaucgagcguuuuagagcuaugcu
	PCR primer for genotyping (forward)	catctaaacggaccctttctgcc
	PCR primer for genotyping (reverse)	gcacgcaaattgtttaccttgagg
<i>goa-1(km98)</i>	crispr RNA	cauggguuguaccaugucaguuuuagagcuaugcu
	PCR primer for genotyping (forward)	gagctgcaccacatacagtgagtg
	PCR primer for genotyping (reverse)	tacaatagtcgattttctgattctcc
<i>gpb-1(H266F)</i>	crispr RNA	aaauuuaucaugagaaucaguuuuagagcuaugcu
	ssDNA	gttcgacattcgctgatcaggaacttgcaatgtatt ctttgataatattatttgcggaatcactagt
	PCR primer for genotyping (forward)	tctccagactccgcacattcatc
	PCR primer for genotyping (reverse)	ttatcgtgaccagccaataactcctg
<i>phip-1(S112A)</i>	crispr RNA	aacauucuuucucuaaugaguuuuagagcuaugcu
	ssDNA	cattttaaagcagaaataccagattataatatccactt cgcgaaacgacggatattgaatctccatggttgagcatagtt
	PCR primer for genotyping (forward)	gtggaatccatgtttaattcccagtggaac
	PCR primer for genotyping (reverse)	gacgctccacaatgtacaatcgtc
<i>phip-1(S112E)</i>	crispr RNA	aacauucuuucucuaaugaguuuuagagcuaugcu
	ssDNA	cattttaaagcagaaataccagattataatatccactt cgaaaacgacggatattgaatctccatggttgagcatagtt
	PCR primer for genotyping (forward)	gtggaatccatgtttaattcccagtggaac
	PCR primer for genotyping (reverse)	gacgctccacaatgtacaatcgtc
<i>3XFLAG::gpb-1</i>	crispr RNA	aaguucgcucaucugcugcguuuuagagcuaugcu
	ssDNA	cgtcgacacttccatcagtaccatcctccggagcagcaccaccacc agcagcaagatggattacaaagaccatgatggtgactat aaggatcatgatattgactataaagacgatgacgataa gagcgaactgaccaactcgcacaggaggctgaacag ctgaagtcgcagattcggg
	PCR primer for genotyping (forward)	aaaacgcgaacaccgaccaggagc
	PCR primer for genotyping (reverse)	attgctagaccatgctctggaacg

**A****B****C****D**

## Appendix Figure S1. Genome editing of *phip-1*, *lhpp-1*, *gpb-1*, and *goa-1*.

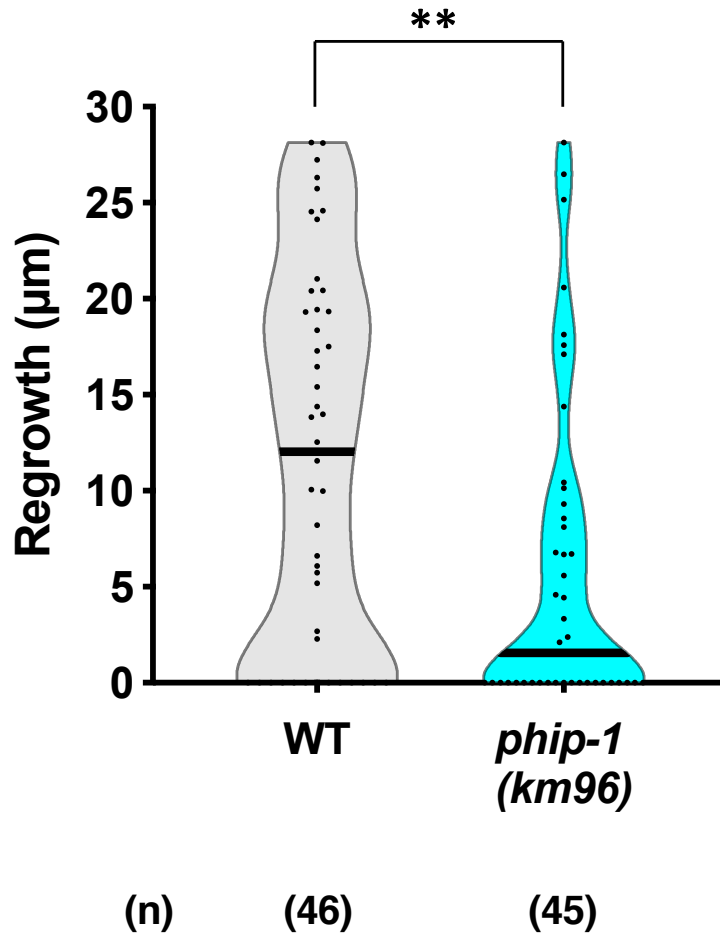
A Genomic structure of the *phip-1* gene. Exons are indicated by boxes, while introns and untranslated regions are indicated by bars. The top and bottom letters indicate nucleotides and corresponding amino acids, respectively. The *phip-1(km96)* mutation is a 14 bp insertion (nucleotides in red) with 1-bp substitution (nucleotide in blue), which causes a frameshift (amino acids in bold) and premature stop codon (\*) in exon 1. The *phip-1(S112A)* and *phip-1(S112E)* alleles are also shown.

- B Genomic structure of the *lhpp-1* gene. The *lhpp-1(km97)* mutation is a 4-bp deletion, which causes a frameshift (amino acids in bold) and premature stop codon (\*) in exon 1.
- C Genomic structure of *gpb-1*. A 3XFLAG epitope tag was inserted into the N-terminus at the endogenous *gpb-1* locus with the CRISPR–Cas9 method. The *gpb-1(H266F)* allele is also shown.
- D Genomic structure of the *goa-1* gene. The *goa-1(km98)* mutation is a 5-bp deletion, which causes a frameshift (amino acids in bold) and premature stop codon (\*) in exon 1.



**Appendix Figure S2. Effect of *phip-1* deletion on the morphology and function of D-type motor neurons.**

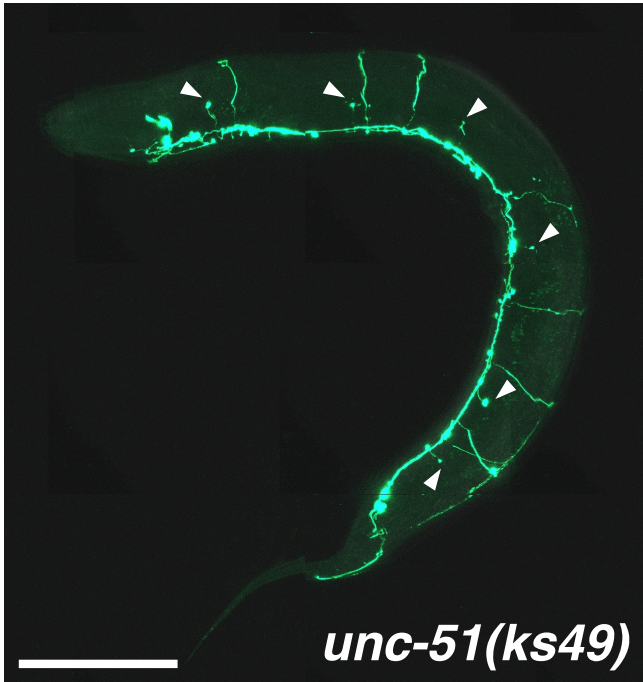
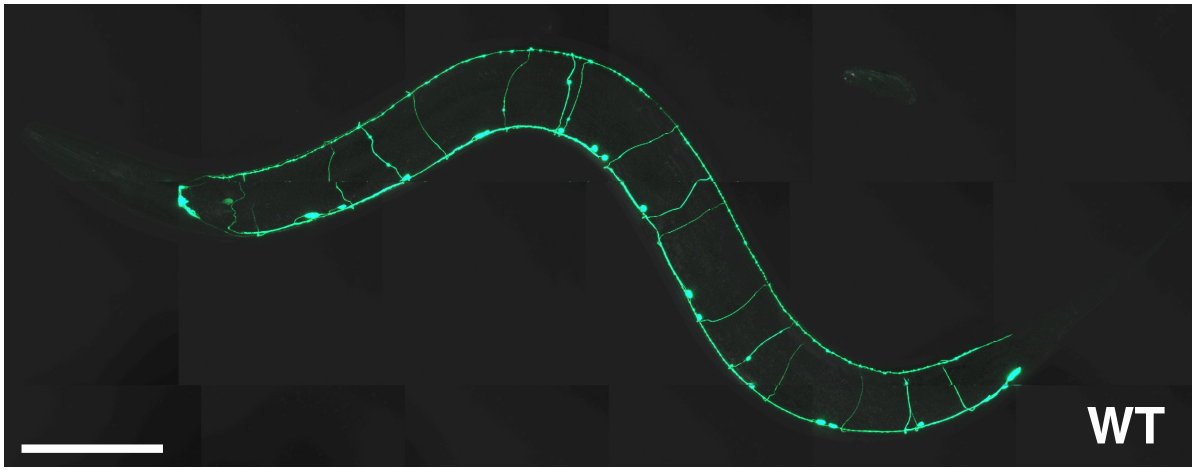
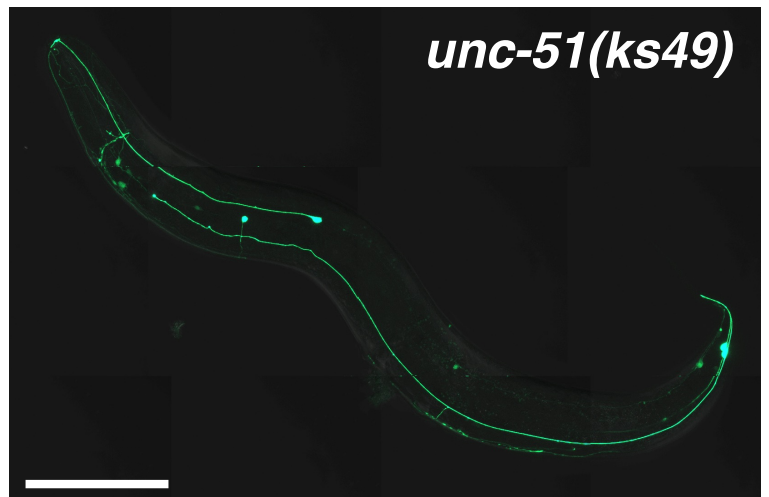
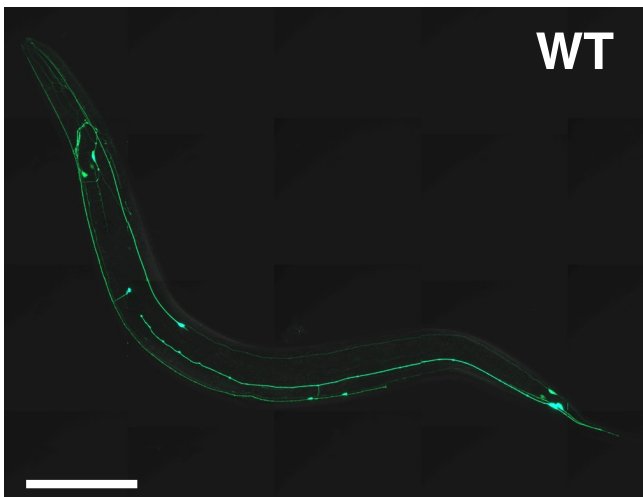
- A** Morphology of D-type motor neurons. Fluorescent images of D-type motor neurons in wild-type and *phip-1(km96)* young adult animals carrying *Punc-25::gfp* are shown. D neurons are visualized by GFP under the control of the *unc-25* promoter. Scale bar, 10  $\mu\text{m}$ .
- B** Aldicarb-induced paralysis assay. The rate of paralysis in wild-type and *phip-1(km96)* animals in the presence of 1 mM aldicarb are shown. Assays were performed blindly and in triplicate. Statistical significance was determined by the log-rank test. Error bars indicate SE.



**Appendix Figure S3. Effect of *phip-1* deletion on the length of D-type motor neurons after laser surgery.**

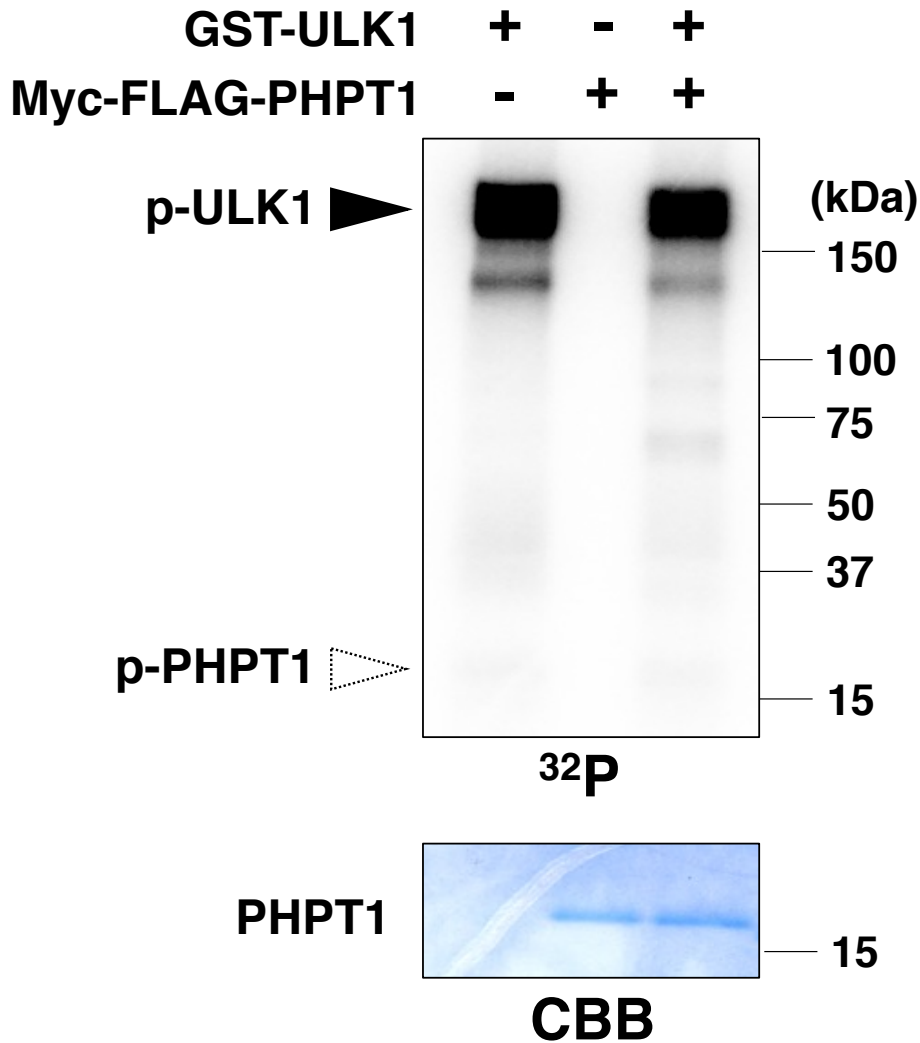
Lengths of regenerating axons 24 h after laser surgery are shown. The number (n) of axons examined is indicated. The black bar in each violin plot indicates the median. \*\* $P < 0.01$ , as determined by the Mann–Whitney test.



**A****B**

**Appendix Figure S4. Effects of the *unc-51* mutation on the development of D-type motor neurons and PLM neurons.**

- A Morphology of D-type motor neurons. Fluorescent images of D-type motor neurons in wild-type and *unc-51(ks49)* young adult animals carrying *Punc-25::gfp* are shown. D neurons are visualized by GFP under the control of the *unc-25* promoter. White arrowheads indicate axons that failed to elongate from ventral to dorsal side during development. Scale bar, 100  $\mu\text{m}$ .
- B Morphology of PLM neurons. Fluorescent images of PLM neurons in wild-type and *unc-51(ks49)* young adult animals carrying *Pmec-7::gfp* are shown. PLM neurons are visualized by GFP under the control of the *mec-7* promoter. Scale bar, 100  $\mu\text{m}$ .

**A****B**

<i>C. elegans</i> PHIP-1	103	<b>KYPDYN</b>	<b>IHF</b>	<b>SNDGY</b>	116	
Human PHPT1	112	<b>KYPDYE</b>	<b>V</b>	<b>TW</b>	<b>NDGY</b>	125

**Appendix Figure S5. ULK1 does not phosphorylate PHPT1 in vitro.**

A Phosphorylation of PHPT1 by ULK1. HEK293 cells were transfected with Myc-FLAG-PHPT1, and cell lysates were immunoprecipitated with anti-FLAG antibodies. Immunopurified PHPT1 was subjected to the in vitro kinase assay with recombinant GST-ULK1 and phosphorylation was detected by autoradiography. Protein input was confirmed by Coomassie Brilliant Blue (CBB) staining. Black arrowhead indicates ULK1 autophosphorylation.

B Sequence alignments of the C-terminal domain of human PHPT1 and *C. elegans* PHIP-1. Identical and similar residues are highlighted with black and gray shading, respectively. Ser-112 (in PHIP-1) and Thr-119 (in PHPT1) are shown.